Translational Control of Apolipoprotein B mRNA: Regulation via Cis Elements in the 5′ and 3′ Untranslated Regions†

Louisa Pontrelli,‡ Konstantinos Gus Sidiropoulos,‡ and Khosrow Adeli*

Department of Laboratory Medicine and Pathobiology, Division of Clinical Biochemistry, Hospital for Sick Children, University of Toronto, Toronto, Ontario M5G 1X8, Canada

Received January 14, 2004; Revised Manuscript Received March 17, 2004

ABSTRACT: Translational control of apolipoprotein B (apoB) mRNA has been previously documented; however, the molecular mechanisms that govern translation of apoB mRNA are unknown. We investigated the role of the untranslated regions (UTR) in the regulation of apoB mRNA translation first by analyzing apoB UTR sequences using M-fold, a program used to predict RNA secondary structure. M-fold analysis revealed hairpin-like elements within the 5′UTR and 3′UTR of apoB mRNA with potential to form stable secondary structure. Luciferase (LUC) reporter assays were conducted to assess the biological activity of the putative RNA motifs within the UTR sequences by transiently transfecting HepG2 cells with chimeric mRNAs containing the 5′ and/or 3′ apoB UTRs linked to a LUC reporter gene. We observed statistically significant increases in LUC activity for the 5′UTRpGL3 and 5′/3′UTRpGL3 constructs. LUC mRNA levels remained constant for all constructs, suggesting that increased LUC activity was likely posttranscriptional in nature. When RNA isolated from transfected cells was translated in vitro, parallel increases in translatable LUC activity were observed. We also examined the role of UTR sequences within the context of the apoB coding sequence, using constructs containing the N-terminal 15% of apoB (apoB15). We observed a 40% and 25% increase in total protein mass with the 5′UTR-apoB15 construct and the 5′UTR-apoB15-3′UTR, respectively, over the control construct with no apoB UTR, with only a slight stimulation observed for apoB15 3′UTR. Radiolabeling analysis of apoB15 synthetic rate showed a more striking 4.5-fold stimulation of protein synthesis by 5′UTR while addition of both UTRs caused a 3.1-fold stimulation over the control construct. Deletion mutant analysis revealed that the stimulatory effect of the 5′UTR on apoB mRNA translation may be dependent on specific hairpin elements formed within the 5′UTR secondary structure. Overall, our data suggest that putative 5′UTR motifs are important for optimal translation of the apoB message whereas the presence of the 3′UTR appears to attenuate wild-type expression. Potential cis−trans interactions of these motifs with putative RNA binding proteins/translational factors are likely to govern apoB mRNA translation and protein synthesis and may play an important role in dysregulation of atherogenic lipoprotein production in dyslipidemic states.

Apolipoprotein B100 (apoB)[1] is an important protein synthesized by the liver that facilitates the transport of very low density lipoproteins (VLDL) and low-density lipoproteins (LDL) in plasma. Increased plasma levels of LDL and LDL-apoB correlate positively with the development of coronary artery disease and atherosclerosis (*1*). ApoB is the sole protein constituent of LDL and also functions as a ligand for the LDL receptor, mediating the uptake and clearance of LDL from plasma (*2*). Acute regulation of apoB secretion appears to occur posttranscriptionally as levels of apoB mRNA remain stable under acute metabolic stimuli (*3*). For example, metabolic states, such as fasting and carbohydrate overloading, alter apoB secretion without altering apoB mRNA levels (*4*). Similarly, oleate and butyrate treatment of HepG2 cells resulted in increased apoB secretion without a change in apoB mRNA levels (*5*−*7*). In addition, an insulin-modulated decrease in the net accumulation of apoB appears to be a result of a posttranscriptional mechanism since apoB mRNA levels were not altered by hormone treatment (*7*, *8*). Thus, apoB regulation appears to occur co- or posttranslationally under most conditions.

Previous studies in our laboratory have investigated the translational control of apoB mRNA. Using a cell-free HepG2 translation system, we were able to show that the translational efficiency of apoB mRNA decreased under insulin treatment and increased under thyroid treatment (*9*,

† This work was supported by an operating grant to K.A. from the Natural Sciences and Engineering Research Council of Canada (NSERC). L.P. was the recipient of the University of Toronto Heart & Stroke/Richard Lewar Centre of Excellence Studentship Award and the Banting and Best Diabetes Centre/Novo Nordisk Studentship Award. K.G.S. is the recipient of the Hospital of Sick Children's Restracomp Scholarship and the Ontario Graduate Scholarship (OGS).

* To whom correspondence should be addressed. Phone: 416-813-8682. Fax: 416-813-6257. E-mail: k.adeli@utoronto.ca.

‡ These authors contributed equally to this work and are listed in alphabetical order.

[1] Abbreviations: UTR, untranslated region; mRNA, messenger ribonucleic acid; LUC, luciferase; apoB, apolipoprotein B100; PCR, polymerase chain reaction; α-MEM, α modification of Eagle's minimum essential medium; DMEM, Dulbecco's modification of Eagle's minimum essential medium; HepG2, human hepatoma cell line; VLDL, very low density lipoprotein; LDL, low-density lipoprotein; SV40, simian virus 40; T_3, 3,3′,5-triiodo-L-thyronine; SDS−PAGE, sodium dodecyl sulfate−polyacrylamide gel electrophoresis; SD, standard deviation.

10.1021/bi049887s CCC: $27.50
Published on Web 05/04/2004

10). Studies in rat hepatocytes also showed insulin-dependent suppression of apoB secretion by a reduction of apoB synthesis as a result of decreased translational efficiency (*11*). Experiments using streptozotocin-induced diabetic rats provided further evidence of apoB mRNA translational control. Decreased apoB synthesis was found to be a direct result of impaired translation rates (*12*). These studies indicate that apoB synthesis may be regulated at the level of translation; however, the molecular mechanisms which mediate translational control of apoB mRNA were not identified.

Translation in eukaryotes is a complex event which can be divided into three stages: (i) initiation, (ii) elongation, and (iii) termination. Initiation of translation is the primary target of translational control. Such control is mainly determined from structural properties of the mRNA, largely in the 5′UTR. It is known, however, that the 3′UTR, interactions between the 5′UTR and 3′UTR, and the coding region may also contribute to the control of mRNA translation (*13*). UTR sequences are known to play crucial roles in the posttranscriptional regulation of gene expression, including modulation of the transport of mRNAs out of the nucleus and of translation efficiency (*14*), subcellular localization (*15*), and stability (*16*).

The focus of our study was to investigate the molecular mechanisms that govern the translational control of apoB mRNA. Sequence and structural elements localized to the 5′ and 3′ untranslated regions (UTR) of mRNAs are known to play significant roles in translational regulation. These regions are defined as cis-regulatory elements. Such elements are known to regulate mRNA translational efficiency and stability and are known to act as binding sites for trans-acting cytoplasmic factors such as translation initiation factors (*17*). ApoB mRNA is 14121 nucleotides long and its 5′UTR and 3′UTR sequences are 128 and 304 nucleotides in length, respectively (*18*). The 5′UTR sequence is relatively GC rich with a 76% composition of G + C nucleotides. It has been identified that GC-rich regions have a high potential for forming stable secondary structure (*19*). Furthermore, studies have shown that highly structured 5′UTR sequences tend to inhibit efficient translation (*19*, *20*). Investigation of the 5′UTR and 3′UTR sequences of apoB mRNA revealed RNA elements with the potential to form stable secondary structure which, in turn, may mediate the translational control of apoB mRNA. By analyzing the 5′UTR, we identified two GC boxes located at positions −20 and −81, upstream of the translational start site, and between these two GC boxes is a GAGGCC doublet; the role of such elements in mRNA translation is not known. The 3′UTR of apoB mRNA also has the potential to form secondary structure and includes sequence elements such as AUUUA and AUUUUUA and AU-rich regions known to play roles in mRNA stability (*13*). We analyzed the potential of the UTR sequences to form secondary structure using M-fold, an RNA secondary structure prediction program. Our primary objective was to determine the biological function of the apoB UTR sequences on the translational efficiency of apoB mRNA and to identify potential cis-regulatory elements.

EXPERIMENTAL PROCEDURES

Cell Culture. HepG2 cells were maintained in complete α-MEM (α modification of Eagle's minimum essential medium). α modification of Eagle's minimum essential medium was obtained from the Media Facility at the Hospital for Sick Children (Toronto, ON, Canada). Medium is prepared using powdered reagents from Gibco/Life Technologies (Toronto, ON, Canada) and is made by the University of Toronto Media Facility. Complete α-MEM medium contained 5% fetal bovine serum and a 1% antibiotic and antimycotic mixture. Cos-7 cells were maintained in DMEM [Dulbecco's modification of Eagle's minimum essential medium; Wisent Labs (Montreal, PQ, Canada)] containing 20% fetal bovine serum. Cells were maintained in a Nuaire incubator at 37 °C under 95% air/5% CO_2. Cells were seeded into T-75 flasks and medium was replenished every 3 days. Cells were subcultured on a weekly basis usually after reaching 90% confluency.

Chimeric UTR-LUC Reporter Constructs. The 5′UTR and 3′UTR transcripts were generated by PCR using apoB18 and apoB100 cDNA, respectively, as templates (kindly provided by Dr. Zemin Yao, University of Ottawa Heart Institute). The primers used to generate the PCR transcripts were designed using the human apoB100 mRNA sequence available through GenBank Accession Number X04506 (*18*). The UTR sequences were cloned into the pGL3 control eukaryotic expression vector (Promega), which contains SV40 promoter and enhancer sequences and the entire sequence encoding the firefly luciferase (LUC) gene. PCR primers were designed such that the 5′ and 3′ flanking regions contained sequences for their respective restriction sites and four extra base pairs to ensure complete enzymatic digestion. All constructs are depicted in Figure 1A. Primer names and sequences used to create all constructs are provided in Table 1A. The first construct contained the apoB 5′UTR cloned upstream of the LUC gene using the *Hin*dIII restriction site (5′UTRpGL3). The second construct contained the apoB 3′UTR cloned downstream of the LUC gene using the *Xba*I restriction site (3′UTRpGL3). The third construct contained both apoB UTR sequences (5′/3′UTRpGL3). This construct was generated by cloning the apoB 5′UTR upstream of the LUC gene into the 3′UTRpGL3 construct. In this case, the 5′UTR PCR product contained *Hin*dIII and *Nco*I sequences at its 5′ and 3′ flanking regions, respectively. The control construct contained the LUC gene with no additional sequences (pGL3 control vector). To ensure that effects observed were due to the specific presence of the apoB UTR sequences, a fourth construct containing a null sequence appropriately positioned was created. This negative control sequence was of equivalent length (128 base pairs) to the apoB 5′UTR and was cloned upstream of the LUC gene using the *Hin*dIII and *Nco*I restriction sites (NC5pGL3) into the 3′UTRpGL3 construct. The sequence was derived from the LUC coding region and corresponded to base pairs 1158−1286 of the pGL3 control vector sequence (Promega). The sequence was examined to ensure that it did not contain any open reading frames or stable secondary structure. All constructs were confirmed by direct DNA sequencing.

Chimeric UTR-ApoB15 Constructs. To generate the UTR-apoB15 constructs, we removed the LUC gene using the *Hin*dIII and *Xba*I restriction sites and inserted the apoB15 coding sequence in its place. The 5′UTR- and/or 3′UTR-apoB sequences were upstream and downstream of the apoB15 coding sequence, respectively (see Figure 3A). Four apoB15 constructs were generated: a control construct

Table 1: Primer Names and Sequences Used for the Chimeric UTR-LUC and UTR-ApoB15 Constructs

construct	primer name	sequence
		(A) Chimeric UTR-LUC Constructs
5′UTRpGL3	FP1−5′	5′-GCGC*AAGCTT*ATTCCCACCGGGACCTGCGGGGCTGAGTGCCCTTC-3′
	RP1−5′	5′-GCGC*AAGCTT*CGCCAGCTGCGGTGGGGCGGCTCCTGGGCTGCGGC-3′
3′UTRpGL3	FP2−3′	5′-GCGC*TCTAGA*TAATTTTTTAAAAGA-3′
	RP2−3′	5′-GCGC*TCTAGA*TATGATACACAATAA-3′
5′/3′UTRpGL3	FP1−5′	5′-GCGC*AAGCTT*ATTCCCACCGGGACCTGCGGGGCTGAGTGCCCTTC-3′
	RP3−5′	5′-GCGC*CCATGG*CGCCAGCTGCGGTGGGGCGGCTCCTGGGCTGCGGC-3′
NC5pGL3	FPNC	5′-GCGC*AAGCTT*CTTCTTCGCCAAAAGCACTC-3′
	RPNC	5′-GCGC*CCATGG*TACCTGGCAGATGGAACCTC-3′
		(B) Chimeric UTR-ApoB15 Constructs
apoB15 control	FP1	5′-GCGC*AAGCTT*ATGGACCCGCCGAGGCCCGCGCTGCTGGCGCTGCT-3′
	RP1	5′-GCGCGC*TCTAGA***TTA**TCCTTCCAAGCCAATCTCGATGAGGTCAGC-3′
5′UTR-apoB15	FP1−5′	5′-GCGC*AAGCTT*ATTCCCACCGGGACCTGCGGGGCTGAGTGCCCTTC-3′
	RP1	5′-GCGCGC*TCTAGA***TTA**TCCTTCCAAGCCAATCTCGATGAGGTCAGC-3′
apoB15 3′UTR	FP2−3′	5′-GCGC*TCTAGA*TAATTTTTTAAAAGA-3′
	RP2−3′	5′-GCGC*TCTAGA*TATGATACACAATAA-3′
5′UTR-apoB15-3′UTR	FP2−3′	5′-GCGC*TCTAGA*TAATTTTTTAAAAGA-3′
	RP2−3′	5′-GCGC*TCTAGA*TATGATACACAATAA-3′

containing the apoB15 sequence alone, a second construct containing the 5′UTR upstream of the apoB15, a third containing the 3′UTR downstream of the apoB15, and a fourth construct containing both UTR sequences appropriately positioned. All primers used to create these constructs were obtained from the DNA Synthesis Facility at the Hospital for Sick Children. Primer names and sequences used to create all constructs are provided in Table 1B.

The apoB15 control construct lacked both the 5′UTR and 3′UTR sequences and was generated by PCR using the apoB18 cDNA as a template. The forward primer contained four extra nucleotides, the *Hin*dIII restriction site, and was designed to anneal from nucleotides 129 (first nucleotide of the coding sequence) to 163 of the apoB mRNA sequence. The reverse primer contained four extra nucleotides, the *Xba*I restriction site, and was designed to anneal to nucleotides 2181−2210, which represents the 15% mark of the apoB mRNA sequence. This primer also contained a stop codon positioned immediately after nucleotide 2210 of the apoB sequence and before the restriction site sequence. The apoB15 PCR product was subcloned into a TA cloning vector (Invitrogen). After positive clones were identified, the apoB15 fragment was removed from the TA cloning vector by restriction digestion with *Hin*dIII and *Xba*I. The fragment was gel purified and ligated with the pGL3 control vector fragment.

The 5′UTR-apoB15 sequence was generated by PCR using the apoB18 cDNA as a template. This sequence contained the 128 nucleotide 5′UTR and 15% of the apoB mRNA coding sequence. The 5′UTR-apoB15 PCR fragment contained *Hin*dIII and *Xba*I sites on the 5′ and 3′ flanking regions, respectively. The 5′UTR-apoB15 PCR product was subcloned into a TA cloning vector (Invitrogen). After positive clones were identified, the 5′UTR-apoB15 fragment was removed from the TA cloning vector by restriction digestion with *Hin*dIII and *Xba*I. The fragment was gel purified and was subsequently ligated with the pGL3 control vector fragment.

The apoB15 3′UTR construct was created by inserting the apoB 3′UTR downstream of the coding sequence into the confirmed apoB15 control construct described above. The 3′UTR was generated by PCR using the same primers described in the UTR-LUC reporter constructs for the 3′UTRpGL3 construct. The 5′UTR-apoB15-3′UTR construct was created using a similar approach. Briefly, the 3′UTR was cloned into the confirmed 5′UTR-apoB15 construct described above. All constructs were confirmed by DNA sequencing.

Expression Studies Using UTR-LUC Reporter Constructs. (A) Transient Transfections of UTR-LUC Reporter Constructs. HepG2 cells were subcultured from T-75 flasks, and 0.4×10^6 cells were seeded per dish into six-well plates. Cells were allowed to attach overnight, and transfection experiments were carried out at 70−80% confluency. Cells were transfected with 0.4 μg of each DNA construct using Effectene transfection reagent by Qiagen. Transfection efficiency was monitored by cotransfecting cells with 0.4 μg of the pRL-TK vector (Promega) that contains the renilla luciferase gene and the HSV-thymidine kinase promoter. This weak promoter is suitable to use as a control as it provides neutral constitutive expression of the renilla luciferase control vector. Firefly LUC and renilla LUC have dissimilar enzyme structures and substrate requirements. Thus, the bioluminescence reactions catalyzed by the firefly LUC (or experimental reporter) and the renilla LUC (control reporter) are quantifiable and discriminate. Cells cotransfected with the various UTR-LUC constructs and the pRL-TK construct were harvested with passive lysis buffer. Activities of each reporter were determined by using the dual-luciferase reporter assay system by Promega. This system allows for sequential measurement of both firefly LUC and renilla LUC activity from a single sample. The reporter or firefly LUC was measured first by adding cell lysate to luciferase assay reagent II (LARII) to generate a luminescent signal which was quantified by a luminometer (Turner Designs Model). A second reagent called Stop & Glow was then added; this reagent quenches the first signal and provides the substrate required to generate a signal from the renilla LUC that is also quantified by the luminometer. A ratio of firefly LUC activity:renilla activity was calculated for each dish to normalize for differences in cell number and transfection efficiency. This value was determined for each construct and allowed for between-experiment comparison.

RNA Isolation and RT-PCR (B). To determine whether observed effects were due to transcripitonal or translational influences, a complement set of dishes was transfected for

RNA isolation. Total RNA was isolated using trizol reagent (Life Technologies) according to manufacturer's instructions. The integrity of isolated RNA was determined by observing the 28S and 18S ribosomal subunits after electrophoresis on agarose gels. LUC mRNA levels for each construct were monitored by performing RT-PCR using the Superscript One-Step RT-PCR system (Life Technologies). Gene-specific primers for the firefly LUC gene were designed; the primers selected had an optimal annealing temperature of 55.4 °C. The forward primer represented base pair 509 to 530 of the LUC coding region, 5′-TCGTCACATCTCATCTACCTCC-3′, and the reverse primer represented base pair 1188 to 1169, 5′-TCTCACACACAGTTCGCCTC-3′, of the LUC coding region within the pGL3 control vector sequence. The reaction resulted in a 680 base pair product. The RT-PCR protocol was performed according to manufacturer's instructions. Briefly, 1 μg of RNA template was added to the reaction mixture and subjected to the following: one cycle of 50 °C for 30 min, 94 °C for 2 min followed by 25 cycles of 94 °C for 15 s, 55 °C for 30 s, and 72 °C for 1 min, and one cycle of 72 °C for 10 min. Products were run on 1% agarose gels and were visualized by staining with Sybr Gold nucleic acid stains. Gels were scanned using the Kodak 1D Digital Science camera, and a net intensity quantitation was determined for each product.

(C) In Vitro Translation. Total RNA species isolated from HepG2 cells transfected with the various chimeric UTR-LUC constructs were subjected to in vitro translation experiments using the Flexi rabbit reticulocyte lysate system by Promega. Since our constructs contained firefly LUC as the reporter, the protocol used was analogous to the conditions suggested for the standard or control LUC RNA translation. Briefly, translation reactions were performed at 30 °C for 90 min after the assembly of all reaction components, including the Flexi Rabbit reticulocyte lysate, amino acids minus methionine (0.01 mM each) and amino acids minus leucine (0.01 mM each), 70 mM potassium chloride, 40 units of RNasin, and 200 ng of RNA template. LUC activity was determined using the luciferase assay system.

(D) Secondary Structure Analysis. The potential for the apoB 5′UTR sequence to form secondary structures such as stem loops or hairpins was assessed by computer analysis using a program called M-fold developed by Zuker (*21*). This program has been used successfully for analysis of other RNA sequences and predicts optimal and suboptimal secondary structures on the basis of free energy minimization (*22*, *23*). This program was used through the Genetics Computer Group (GCG) available through the bioinformatics web site at the Hospital for Sick Children. The program was run using the default parameters set by the program.

(E) Chimeric UTR Deletion Mutant-LUC Reporter Constructs. The 5′UTR deletion mutant constructs were generated by PCR using apoB15 cDNA as a template (kindly provided by Dr. Zemin Yao, University of Ottawa Heart Institute). Primers used for the PCR reactions containing *Hin*dIII restriction sites are shown in Table 2. The whole apoB 5′UTR was generated using primers *Hin*dIII-1F and *Hin*dIII-128R. Deletion mutant 1−64 was amplified using PCR primers *Hin*dIII-1F and *Hin*dIII-64R. PCR for deletion mutant 1−96 was conducted using *Hin*dIII-1F and *Hin*dIII-96R. Deletion mutant 32−128 was generated using PCR primers *Hin*dIII-32F and *Hin*dIII-128R. The 5′UTR fragment 64−128 was amplified using primers *Hin*dIII-64F and *Hin*dIII-128R. The PCR products were subcloned into pCR 4-TOPO using the TOPO TA cloning kit for sequencing (Invitrogen) following the manufacturer's instructions. The UTR sequences were digested from the TOPO vectors after sequencing and were cloned into the pGL3 control eukaryotic expression vector (Promega) at the *Hin*dIII multiple cloning site. The direction of insertion was assessed by sequencing.

Table 2: Primer Names and Sequences Used for the 5′UTR Deletion Mutant Constructs

primer name	primer sequence
*Hin*dIII-1F	GCCGAAGCTTATTCCCACCGGGACCTGC
*Hin*dIII-64R	GCCGAAGCTTTGGGCGGGCTCCTCCGCG
*Hin*dIII-96R	GCCGAAGCTTGGCCTGGCCTCGGCCTCG
*Hin*dIII-32F	GCCGAAGCTTTCTCGGTTGCTGCCGCTGAG
*Hin*dIII-128R	GCCGAAGCTTCGCCAGCTGCGGTGGGGC
*Hin*dIII-64F	GCCGAAGCTTGCCAGCCAGGGCCGCGAG

Expression Studies Using the UTR-ApoB15 Constructs. (A) Transient Transfection Experiments. Cos-7 cells were transfected with 1 μg each of the various UTR-apo B15 constructs using lipofectamine. The cells were lysed 48 h posttransfection in lysis buffer (phosphate-buffered saline containing 1% Nonidet P-40, 1% deoxycholate, 5 mM EDTA, 1 mM EGTA, 2 mM PMSF, 0.1 mM leupeptin, and 2 μg/mL *N*-acetylleucinylleucinylnorleucinal) and were passaged through a syringe to homogenize.

(B) Chemiluminescent Immunoblot Analysis. Cell samples, either directly or after immunoprecipitation against a target protein, were subjected to chemiluminescent immunoblotting for apoB using 1D1 monoclonal antibody (kindly provided by Dr. Ross Milne, University of Ottawa). Samples were analyzed by SDS−PAGE using 8% polyacrylamide minigels (8 × 5 cm). Following SDS−PAGE, the proteins were transferred electrophoretically overnight at 4 °C onto poly(vinylidene difluoride) membranes using a Bio-Rad wet transfer system. The membranes were blocked with a 5% solution of fat free dry milk powder, incubated with antiserum, washed, and then incubated with a secondary antibody conjugated to peroxidase. Membranes were then incubated in an enhanced chemiluminescence detection reagent (Amersham Pharmacia Biotech) for 60 s and exposed to Eastman Kodak Co. hyperfilm. Films were developed, and quantitative analysis was performed using an imaging densitometer.

(C) Metabolic Radiolabeling of ApoB15. Cos-7 cells transfected with the chimeric UTR-apoB15 constructs were preincubated in methionine-free Dulbecco's minimum essential medium at 37 °C for 1 h and labeled with 100 μCi/mL [^{35}S]methionine for 30 min 2 days posttransfection. Following the labeling pulse, the cells were washed twice and harvested by lysis in solubilization buffer (phosphate-buffered saline containing 1% Nonidet P-40, 1% deoxycholate, 5 mM EDTA, 1 mM EGTA, 2 mM PMSF, 0.1 mM leupeptin, and 2 μg/mL *N*-acetylleucinylleucinylnorleucinal). The lysates were centrifuged for 10 min at 4 °C in a microcentrifuge (12000 rpm), and supernatants were collected for immunoprecipitation.

(D) Immunoprecipitation, SDS−PAGE, and Fluorography. Immunoprecipitation was performed as described previously (*24*) using goat anti-human apoB antibody. Immunoprecipitates were washed with wash buffer [10 mM Tris-HCl (pH

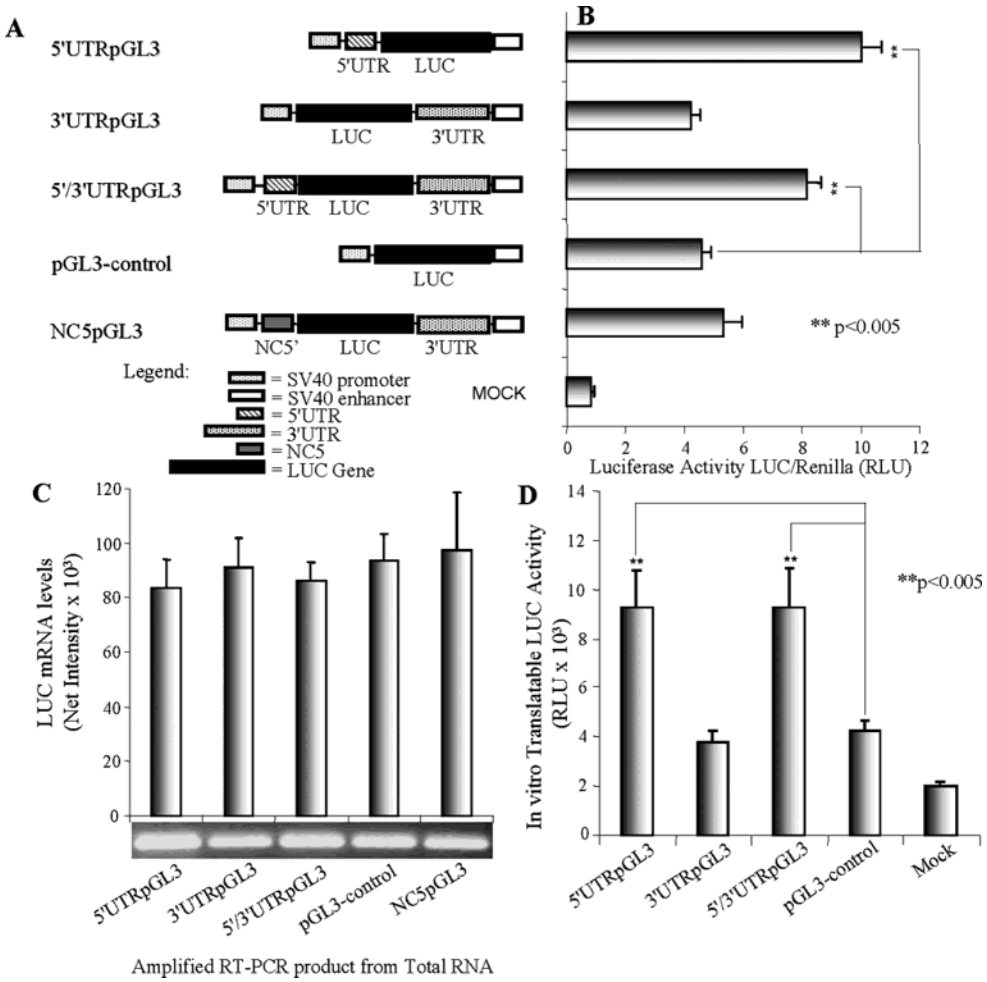

FIGURE 1: (A) Chimeric UTR-LUC constructs carrying the 5′UTR and/or 3′UTR of apoB mRNA. The 5′UTR and 3′UTR sequences of apoB mRNA were generated by PCR. The 5′UTRpGL3 construct was created by cloning the 5′UTR upstream of the LUC gene using the *Hin*dIII restriction site. The 3′UTRpGL3 construct was created by cloning the apoB 3′UTR downstream of the LUC gene using the *Xba*I restriction site. The 5′/3′UTRpGL3 construct was created by cloning the 5′UTR upstream of the LUC coding region using the *Hin*dIII and *Nco*I restriction sites into the 3′UTRpGL3 construct. The pGL3 control construct contained no apoB UTR sequences. The negative control construct (NC5pGL3) carried a null sequence derived from the LUC gene itself and was equivalent in length to the apoB 5′UTR. This was cloned upstream of the LUC gene using the *Hin*dIII and *Nco*I restriction sites into the 3′UTRpGL3 construct. (B) Transient transfection of HepG2 cells with the chimeric UTR-LUC constructs. HepG2 cells were transiently cotransfected with the chimeric apoB UTR-LUC constructs (panel A) and the pRL-TK (renilla LUC) vector (see Experimental Procedures). Cells were harvested 48 h posttransfection, and LUC activity was assessed using the dual LUC assay system. Transfection efficiency for each dish was normalized by dividing firefly LUC activity by renilla LUC activity. Mean ± SEM luciferase values are from 12 independent experiments performed in triplicate. (C) Assessment of LUC mRNA levels following transient transfection of the chimeric UTR-LUC constructs. LUC mRNA levels were assessed by RT-PCR (see Experimental Procedures). RNA products used for RT-PCR reactions were isolated following transient transfection of HepG2 cells with the various chimeric UTR-LUC constructs. RT-PCR products were run on agarose gels, stained with Sybr Gold, and were scanned using the Kodak 1D Digital Science camera; a net intensity quantitation was determined for each product. Mean ± SEM luciferase mRNA values are from seven independent RNA isolation experiments. RNA was isolated from seven independent experiments in which each construct was transfected in triplicate. A representative scan of one RT-PCR experiment is displayed. (D) In vitro translation of RNA products derived from transient transfection of HepG2 cells with the chimeric UTR-LUC constructs. Isolated RNA products (200 ng) from transient transfection of HepG2 cells with the various chimeric UTR-LUC constructs were translated in vitro (see Experimental Procedures). Measuring LUC activity of the lysate assessed translatability of RNA for each construct. Mean ± SEM luciferase values are from six independent RNA samples in vitro translated in duplicate. RNA was isolated from six independent experiments in which each construct was transfected in triplicate.

7.4), 2 mM EDTA, 0.1% SDS, 1% Triton X-100] and prepared for SDS−PAGE by resuspension and boiling in 100 μL of electrophoresis sample buffer. SDS−PAGE was performed essentially as described (*25*). The gels were fixed and saturated with Amplify (Amersham Pharmacia Biotech) before being dried and exposed to Dupont autoradiographic film at −80 °C for 1−4 days. ApoB15 bands were excised from the gel, digested in hydrogen peroxide/perchloric acid, and associated radioactivity was quantified by liquid scintillation counting.

RESULTS

Construction of UTR-Reporter and UTR-ApoB15 Vectors. The different chimeric UTR-LUC constructs used in the present analysis are displayed in Figure 1A. Each contained a SV40 promoter and enhancer sequences as well as the LUC coding sequence with the apoB 5′UTR and/or 3′UTR inserted as indicated. The negative control construct (NC5pGL3) contained a null sequence derived from the LUC coding sequence and was positioned upstream of the LUC gene (as in the 5′/3′UTRpGL3 construct). The chimeric UTR-apoB15

constructs used in the present analysis are displayed in Figure 1A. The pGL3 vector backbone remained analogous to that used in the reporter constructs except that the LUC gene was removed and replaced by 15% of the coding sequence for apoB. The apoB 5′UTR and/or 3′UTR were (was) positioned upstream and downstream of the apoB15 sequence as indicated.

Influence of the ApoB 5′UTR and 3′UTR on LUC Expression. By assaying for LUC activity expressed in each set of transfectants, we evaluated the influence of apoB UTR sequences on LUC expression of chimeric transcripts carrying those sequences. To normalize for transfection efficiency and cell viability after transfection, we employed the dual luciferase reporter assay system (see Experimental Procedures). All experiments were performed in triplicate; a mean was calculated for each construct, and the fold increase/decrease in LUC activity versus control was determined. Figure 1B summarizes the results obtained. We observed a statistically significant 2.2-fold increase ($p < 0.005$) in LUC activity from the chimeric construct carrying the apoB 5′UTR cloned upstream of the LUC gene (5′UTR-pGL3) in comparison to the pGL3 control construct. We did not observe any significant difference in LUC activity from the construct carrying the 3′UTR alone (3′UTRpGL3) in comparison to the control. The construct carrying both UTRs (5′/3′UTRpGL3) exhibited a significant 1.8-fold increase in LUC activity in comparison to control ($p < 0.005$). These data suggest that while the apoB 5′UTR sequence is required for its optimal expression, the 3′UTR on its own does not appear to play a crucial role. The presence of both the 5′UTR and 3′UTR of apoB appeared to result in an increase in LUC activity as compared to that observed with the 5′UTR alone. However, the increase in LUC activity observed with the 5′/3′UTRpGL3 construct was 1.8-fold versus a 2.2-fold increase with the construct carrying the 5′UTR alone. Statistical analysis comparing the LUC activity measured from the 5′UTRpGL3 and the 5′/3′UTRpGL3 constructs (1.8-fold versus 2.2-fold) showed a significant difference ($p = 0.04$). This may suggest that the presence of the 3′UTR slightly attenuated the stimulatory effect observed with the 5′UTRpGL3 construct. The LUC activity results obtained from cells transfected with the negative control construct (NC5pGL3) were comparable to the LUC activity derived from the pGL3 control construct. This suggests that the increased LUC activity observed in the 5′UTRpGL3 and 5′/3′UTRpGL3 constructs was sequence specific and not simply due to the presence of an additional sequence upstream of the LUC gene.

Determination of LUC mRNA Levels from Transfected Cells. Total RNA isolated from the HepG2 cells transfected with the various UTR-LUC constructs was used for RT-PCR experiments in order to identify whether the increase in LUC activity was due to transcriptional or co- or posttranslational control. The RT-PCR reaction was carried out according to the instructions provided with the Superscript One-Step RT-PCR kit by Gibco/Life Technologies (see Experimental Procedures). The cycle number was optimized to 25 cycles in order to ensure that the RT-PCR reaction had not reached a plateau resulting in consistent band intensities for each construct. At 20 cycles appreciable product formation did not occur for the constructs; however, LUC mRNA levels were detected with the pGL3 control vector. The cycle number was subsequently changed to 25 cycles, and this was selected as the target cycle number as it allowed sufficient time for detection of LUC mRNA levels for all experimental constructs and the control vector. Statistical analysis indicates that LUC mRNA levels determined from each of the chimeric constructs containing the UTR sequences did not significantly increase or decrease in comparison to the pGL3 control vector (Figure 1C). These results suggest that the increase in LUC activity was likely due to co- or posttranslational regulation and not due to transcriptional upregulation of the constructs containing the apoB 5′UTR sequence.

Influence of the ApoB 5′UTR and 3′UTR on Translational Efficiency in Vitro. Total RNA from HepG2 cells transfected with each chimeric construct was isolated and used for in vitro translation experiments using a rabbit reticulocyte lysate system (see Experimental Procedures). The results obtained from these experiments are depicted in Figure 1D. The results paralleled the transfection data in that we observed an increase in LUC activity with constructs containing the apoB 5′UTR sequence. The construct containing the 5′UTR alone exhibited a statistically significant 2.2-fold increase in LUC activity over the control construct ($p < 0.005$). The LUC activity obtained from the 3′UTRpGL3 construct was not significantly different in comparison to the pGL3 control construct. Similar to the 5′UTRpGL3 construct, the 5′/3′UTRpGL3 construct (carrying both UTRs) exhibited a 2.2-fold increase in LUC activity in comparison to the pGL3 control construct ($p < 0.005$). These results suggest that the presence of the apoB 5′UTR stimulated an increase in in vitro translation of LUC mRNA, suggesting a role in translational control.

Influence of the ApoB 5′UTR and 3′UTR on ApoB15 Expression: Total Protein Mass. To determine the effect of the untranslated regions on apolipoprotein B total protein mass expression, we conducted immunoblotting experiments on Cos-7 cells transfected with the chimeric apoB15. As shown in Figure 2B, the 5′UTR-apoB15 construct exhibited the highest level of expression with a 40% increase in total protein mass over the apoB15 control vector which did not possess any UTR regions ($p < 0.01$). The apoB15 protein mass was slightly (11%) increased with the apoB15 3′UTR construct over control levels ($p = 0.054$). The 5′UTR-apoB15-3′UTR "wild-type" vector containing both UTRs induced a 25% increase in apoB15 protein mass over control levels ($p < 0.01$). It thus appeared that the presence of the 3′UTR reduced the stimulatory effect of 5′UTR on apoB15 synthesis.

Influence of the ApoB 5′UTR and 3′UTR on the ApoB15 Synthetic Rate. We assessed the function of the UTRs on the synthetic rate of newly synthesized apoB mRNA by conducting radiolabeled pulse experiments in Cos-7 cells transfected with the chimeric UTR-apoB15 constructs. As illustrated in Figure 2C, the results resemble the total protein mass experiments; however, the differences are greater. The 5′UTR-apoB15 construct exhibited a 5-fold increase in translation relative to the apoB15 control construct containing no UTR sequences ($p < 0.001$). Elimination of the 3′UTR (5′ apoB15) from the wild-type 5′ apoB15 3′ construct resulted in a 1.4-fold increase in newly synthesized apoB ($p < 0.01$). The 5′UTR-apoB15-3′UTR wild-type construct exhibited a 2.7-fold increase in translation over the apoB15 control construct which possessed no UTRs ($p < 0.01$).

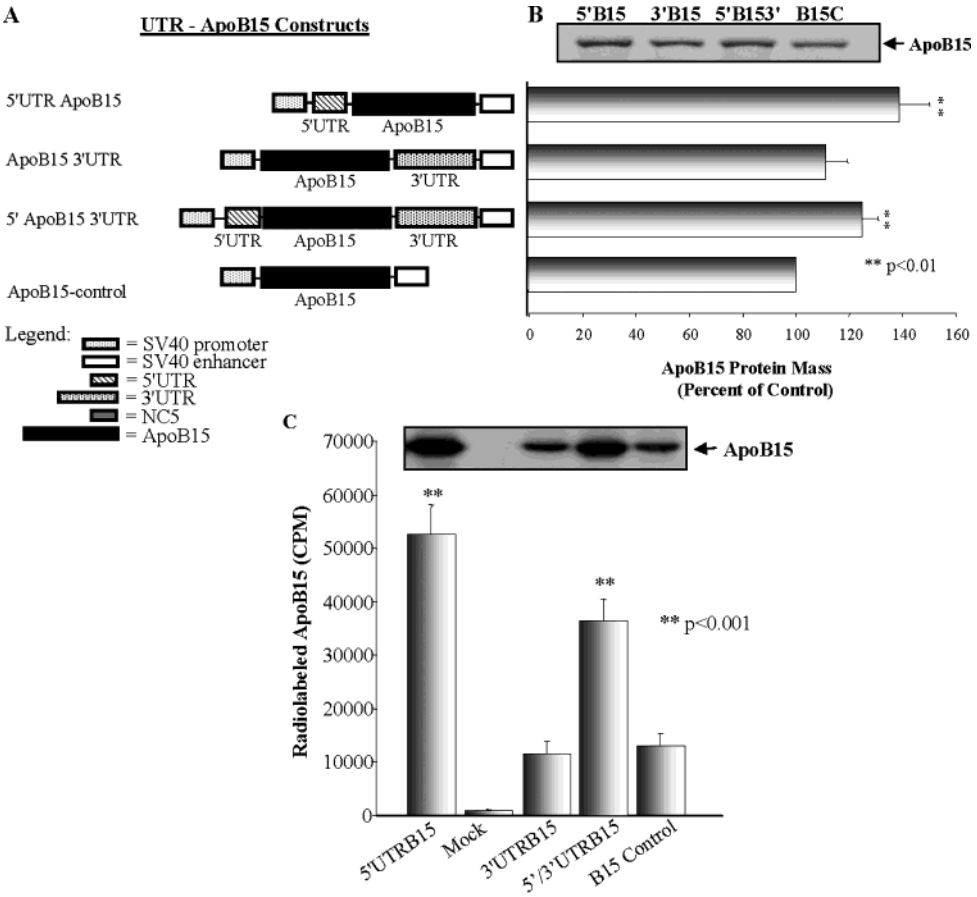

FIGURE 2: (A) Chimeric UTR-apoB15 constructs carrying the 5′UTR and/or 3′UTR of apoB mRNA. The UTR-apoB15 constructs are identical to the UTR-LUC constructs with the exception that they have the apolipoprotein B15 gene (the first 15% of the coding region) in place of the luciferase gene. The apoB15 sequence was generated by PCR, and primers were designed to carry the *Hin*dIII and *Xba*I restriction sites. The 5′UTR-apoB15 construct was also generated by PCR using primers carrying the *Hin*dIII and *Xba*I restriction sites. These products were subsequently cloned into the vector fragment of the pGL3 control vector (with the LUC gene removed). The apoB15 3′UTR construct was generated by cloning the apoB 3′UTR sequence into the apoB15 control construct, downstream of the coding sequence. The 5′UTR-apoB15-3′UTR construct was generated by cloning the apoB 3′UTR into the 5′UTR-apoB15 construct downstream of the coding sequence. (B) Effect of UTRs on apoB15 total protein mass. Cos-7 cells were transfected with the UTR-apoB15 constructs as described (see Experimental Procedures). The cell lysates were run on a SDS−PAGE gel, transferred onto a PVDF membrane, and immunoblotted for apoB using 1D1, an N-terminal-specific monoclonal apoB antibody. Films were developed, and quantitative spot densitometry analysis was performed using an imaging densitometer. Data were plotted from imaging densitometry analysis of four separate experiments in triplicate (shown as mean ± SD). A scan of one representative experiment is displayed. (C) Effect of UTRs on apoB15 synthetic rate. Cos-7 cells were transfected with UTR-apoB15 constructs and were pulsed with [^{35}S]methionine for 30 min 48 h posttransfection. Cells were solubilized, and cell extracts were subjected to immunoprecipitation by a specific anti-apoB antibody and were then analyzed by SDS−PAGE and fluorography. A representative fluorograph is shown, and the data are plotted from imaging densitometry analysis of four separate experiments in triplicate (shown as mean ± SD).

Elimination of the 5′UTR from the 5′ apoB15 3′ wild-type construct resulted in a 2.77-fold reduction in newly synthesized apoB15 ($p < 0.001$). The synthetic rate of apoB15 3′UTR translation was not significantly different than that of the apoB15 control construct (no UTRs).

Secondary Structure Predictions of the ApoB 5′UTR. The computer program M-fold generated five secondary structure predictions of the apoB 5′UTR sequence; these are depicted in Figure 3. The Gibbs free energy of formation determined for each prediction was in the range of −51.2 to −52.8 kcal/mol. The calculated values suggest that structures formed by the apoB 5′UTR are stable. Structural analysis of each prediction revealed that all of the five predictions (3A−3E) possess a Y-shaped structure. Each branch of the "Y" is composed of two stem loops. All of the structures have three discernible stem-loop structures which they all share in common to some degree. From the 5′ end, a stem loop (stem loop I) exists from nucleotides 3 to 13 in all the structures, with a Gibbs free energy of formation of −4.7 kcal/mol. Stem loop II is the next stem loop from the 5′ end and has two variations. The first variation (stem loop II-S) has a Gibbs free energy of formation of −7.1kcal/mol and is found in structures 3A and 3B at nucleotides 48−66. The second variation (stem loop II-L) is larger and more stable with a Gibbs free energy of formation of −23 kcal/mol and is found in three of the five structures (3C−3E) at nucleotides 21−67. A third stem loop (stem loop III) is found in four of the five structures. It is located at nucleotides 69−90, with a Gibbs free energy of −16 kcal/mol. Structure 3E has a different stem loop III (stem loop III−V) from nucleotides 73 to 103. Furthermore, four of the structures (3B, 3D, and 3E) have a fourth and final stem loop which is variable in all of the structures.

Minimal Sequence of the Human ApoB 5′UTR Necessary for a High Level of Reporter Expression. To determine the minimal sequence or secondary structure of the 5′UTR

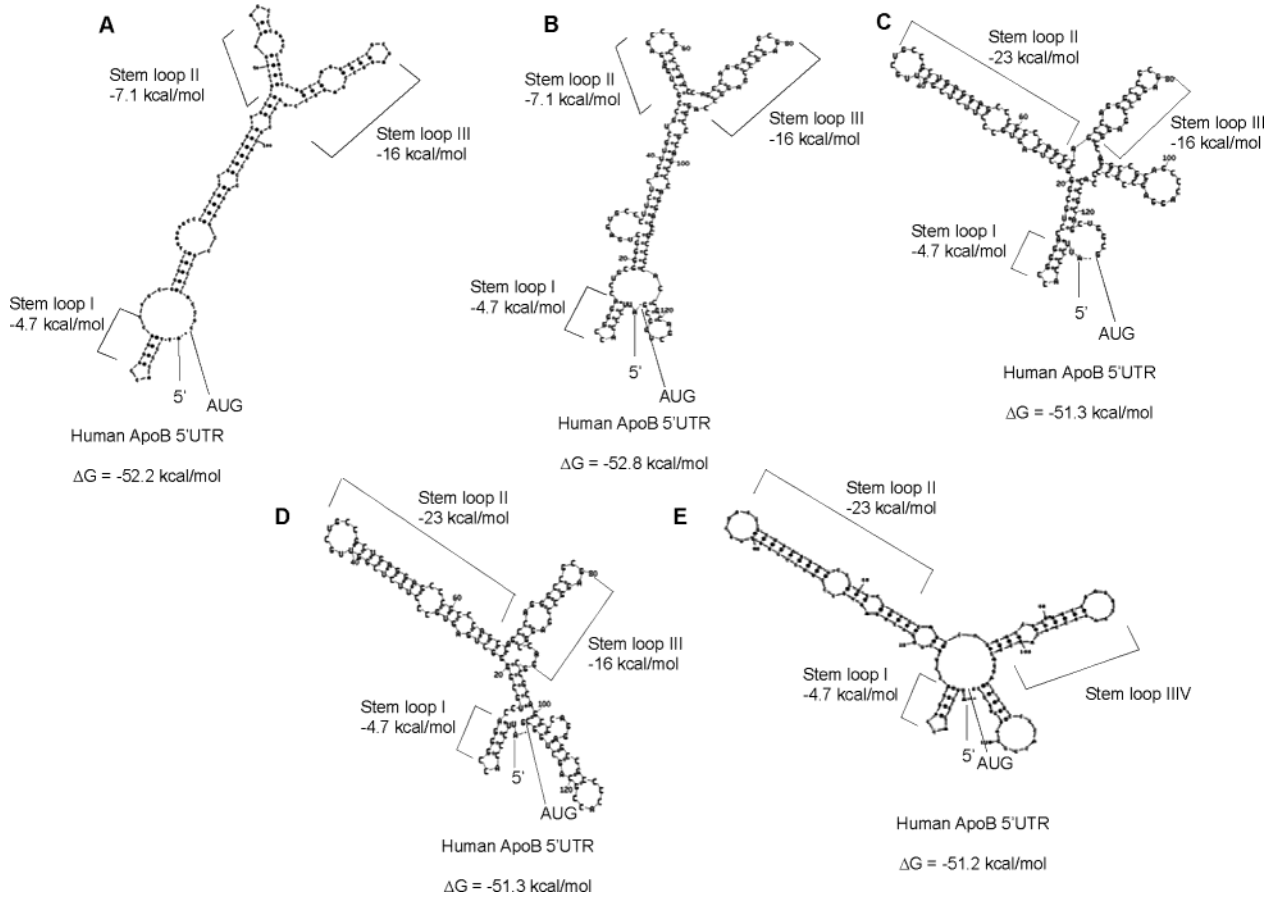

FIGURE 3: Secondary structure analysis of apoB 5′UTR using M-fold. Secondary structure predictions of the apoB 5′UTR sequence were obtained from the program M-fold (see Experimental Procedures). The ΔG calculated for each prediction was in the range of −51.2 to −52.8 kcal/mol.

required for the observed translational effects, several constructs containing various 32 nucleotide deletions of the 128-nucleotide 5′UTR were cloned upstream of the luciferase gene in the pGL3 control vector (see Figure 4A). The construct lacking the apoB 5′UTR had a 2.5-fold expression over background levels (see Figure 4B). The wild-type construct with the full 1−128 sequence had the highest level of expression, with a 7-fold increase over background levels and a 2.7-fold increase over the construct without the apoB 5′UTR ($p < 0.05$). Deletion of the first 32 nucleotides (32−128 construct) caused a significant loss of luciferase expression similar to background levels ($p < 0.05$). Deletion of the first 64 nucleotides of the 5′UTR (construct 64−128) resulted in expression levels similar to that of the construct lacking the 5′UTR ($p < 0.05$). Similarly, deletion of the last 64 nucleotides (construct 1−64) resulted in expression levels similar to that of the construct lacking the 5′UTR ($p < 0.05$). Deletion of the last 32 nucleotides (construct 1−96) had no appreciable effect on luciferase activity compared to that of the construct carrying the wild-type "1−128" 5′UTR (approximately 7-fold over background levels or 2.7-fold over pGL3 control levels, $p < 0.05$).

Secondary Structure Predictions of the Deletion Mutants of the ApoB 5′UTR. Secondary structure analysis of the deletion mutant fragments of the apoB 5′UTR was performed using the M-fold program (Figure 5). For the 5′UTR 1−96 construct, two structures were predicted, both of which retained all common stem loops I, II-L, and III of the wild-

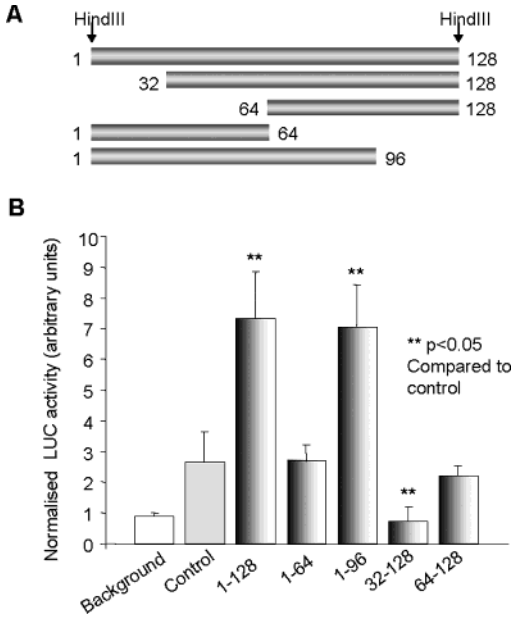

FIGURE 4: Deletion mutant analysis of the apoB 5′UTR. The apoB 5′UTR deletion mutant constructs were generated by PCR, and primers were designed to carry *Hin*dIII restriction sites. The 5′UTR-apoB15 construct was also generated by PCR using primers carrying the *Hin*dIII restriction sites. These products were cloned into the pGL3 control vector. Deletion mutants of the apoB 5′UTR were cloned upstream of the coding sequence of the luciferase gene using *Hin*dIII restriction sites (A). HepG2 cells were transfected with these constructs, and LUC activity was measured. Relative Fluc/Rluc activities were determined (B).

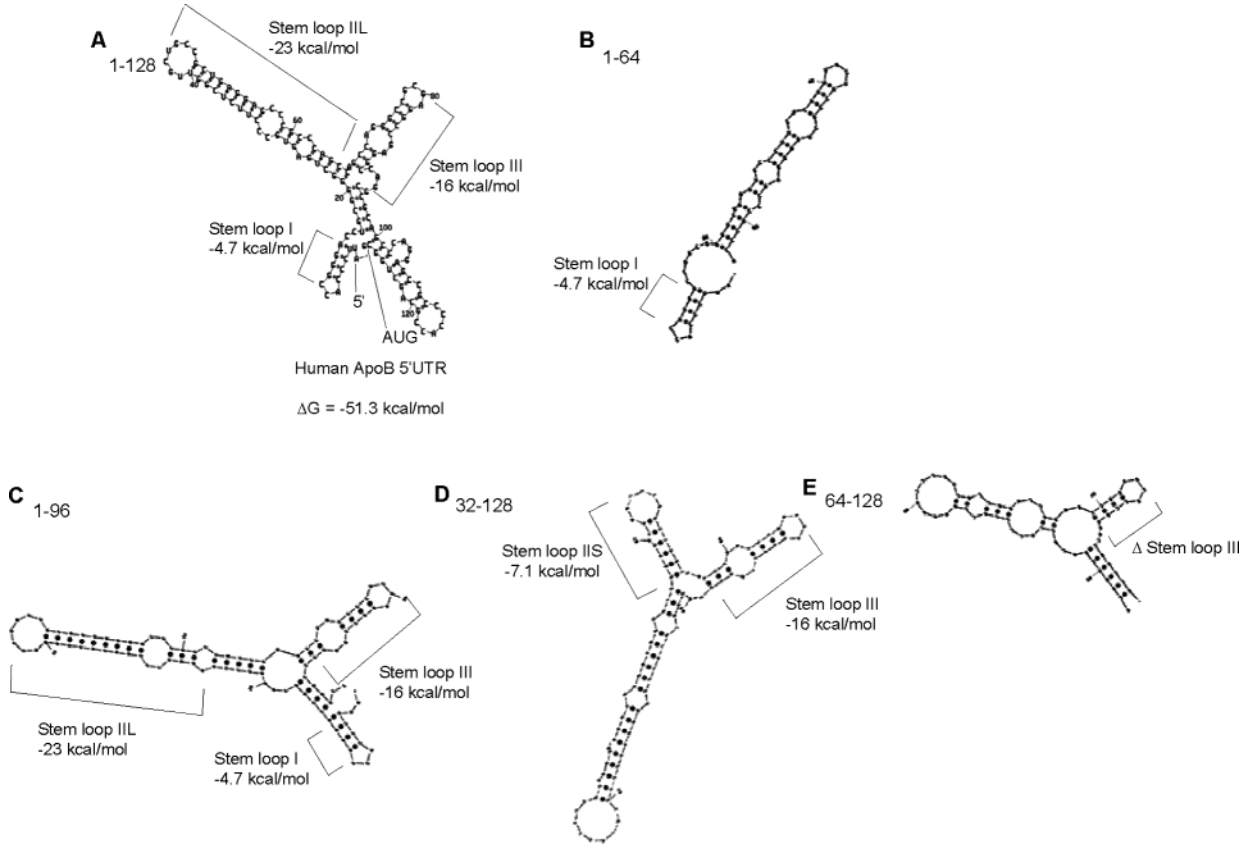

FIGURE 5: Predicted secondary structures of the apoB 5′UTR deletion mutants. Secondary structure predictions were obtained from the program M-fold for four of the apoB 5′UTR deletion mutant constructs (B−E). The predicted secondary structure of the entire apoB 5′UTR 1−128 is included for comparison (A).

type 5′UTR 1−128 structure. The 32−128 construct only retained stem loops II-S and III of the wild-type 5′UTR structure in four of the five predicted structures. In addition, one of the 32−128 structures contained stem loop II-L only. The 1−64 construct preserved the small hairpin I of the wild-type 5′UTR in all of its predicted secondary structures. The 64−128 construct retained only a part of hairpin III in all of its predicted secondary structures.

DISCUSSION

Molecular mechanisms involved in the regulation of apoB mRNA translation have not been extensively studied. Sequence and structural elements within the apoB UTRs suggest that these sequences may participate in modulation of apoB mRNA translation. The focus of our study was to address the role of the 5′UTR and 3′UTR in translational control of apoB mRNA. Biological activity of the apoB UTR sequences was initially investigated by transiently transfecting HepG2 cells with chimeric DNA constructs containing the 5′UTR and/or 3′UTR linked to a firefly luciferase (LUC) reporter gene. We further investigated the biologically activity of the UTR sequences by transiently transfecting Cos-7 cells with similar DNA constructs containing the apoB 5′UTR and/or 3′UTR sequences linked to a truncated portion (15%) of the coding region for apoB100, the protein of interest.

The luciferase reporter data revealed that the 5′UTR plays an important role in the translation of the reporter mRNA as was demonstrated in the 2.2-fold increase in LUC activity as compared to the pGL3 control vector. Furthermore, LUC activity of the 5′/3′UTRpGL3 construct (1.8-fold over control) was also slightly lower than the 5′UTRpGL3 construct, indicating that the 3′UTR may decrease the translation of apoB mRNA. The negative control construct (NC5pGL3) exhibited LUC activity essentially equivalent to the pGL3 control construct. This provided evidence for the sequence or structural specificity of the 5′UTR in mediating expression of the apoB mRNA. These results indicate that the presence of the 5′UTR is essential for optimal translation of the apoB message.

The concentration and activity of the expressed RNA from the reporter experiments were also assessed using RT-PCR and in vitro translation experiments. Luciferase mRNA levels did not significantly change from one construct to another, thus implying that the increase in LUC activity was likely posttranscriptional in nature. In vitro translation of RNA products derived from transfected cells also provided evidence for posttranscriptional modulation as an increase in translatable LUC activity was observed from RNA derived from cells transfected with constructs that contained the 5′UTR sequence. Taken together, the results obtained from cell culture and in vitro experiments provide support for the notion that the 5′UTR plays an important role in optimal translation of apoB mRNA.

Interestingly, the in vitro translation data indicate that in a cell free system the 5′/3′ pGL3 construct is able to translate the mRNA as efficiently as the construct containing the 5′UTR alone since both exhibited equivalent values in translatable LUC activity. This led us to postulate that there may be factors present in the cytoplasm of transfected cells

which are able to bind to the 3′UTR in conjunction with the 5′UTR of the 5′/3′ construct and modulate its translation.

Data derived from the UTR-apoB15 constructs allowed for a direct assessment of the roles of the apoB UTR sequences in translation within the context of the coding region of the protein of interest. In the first series of experiments, we investigated the effect of the UTRs on apoB15 total protein mass over the period of 2 days. The data obtained from these experiments paralleled and therefore confirmed the results observed from the reporter constructs. The construct carrying the 5′UTR alone allowed for the highest amount of translation whereas the constructs carrying the 3′UTR alone showed a decrease in the amount of translation to little above that observed from apoB15 control construct levels. The construct carrying both UTR sequences exhibited a translational efficiency that is close to but below that of the construct carrying the 5′UTR alone.

Interestingly, the effects of the UTR regions on translation were more pronounced when we examined the in vitro apoB15 synthetic rate in a pulse experiment over a 30 min period. The 5′UTR-apoB15 construct induced apoB15 synthesis five times more efficiently than the apoB15 control construct (no UTRs) or the 3′UTR-apoB15 construct. The wild-type construct (5′UTR-apoB15-3′UTR) exhibited translational efficiency that was four times higher over control levels. Thus the radiolabeling protocol appeared to be a more sensitive measure of translational efficiency as compared to the measurement of total protein mass.

The 5′UTR of apoB is a short 128-nucleotide sequence. The leader sequence is GC rich with 76% of its length consisting of G + C residues. The 5′UTR of apoB does not contain any upstream AUG codons. Its AUG codon occurs at position 1 of the protein coding sequence. The context surrounding the AUG codon is favorable (ggcgAUGgac) as it has a G present at positions −3 and +4 (*19*). Since the authentic AUG codon is in a good context we assume that recognition by the Met-tRNA occurs efficiently. Sequences which are GC rich have a tendency to form stable secondary structures. Results obtained from analysis of the 5′UTR using the computer program M-fold predict a free energy of formation in the range of −50.5 to −52.8 kcal/mol. A ΔG value in this range is indicative of the potential to form very stable secondary structures and would likely result in inefficient translation due to inability of the ribosomal complex to unwind the secondary structure and reach the AUG codon (*20*). M-fold results indicated that most stem loops (II and III) occurred within the central region of the apoB 5′UTR from nucleotides 21−67 or 48−66 and 69−90; stem loops in central regions may interfere with the scanning of the 40S ribosomal complex (*26*). This suggests that the 5′UTR should result in an inhibition of translation; however, this is not what we observed in our cell culture and in vitro experiments. Our findings challenge some of the literature published which suggests that most highly structured 5′UTRs lead to an inhibition of translation. However, a recent paper by Vivinus et al. (*27*) on the human heat shock protein 70 (Hsp70) describes the first report of a 5′UTR with a high degree of stable secondary structure (predicted ΔG of ∼−70 kcal/mol) to confer increased translational efficiency of Hsp70 mRNA translation. The presence of the 213-nucleotide GC-rich human Hsp70 5′UTR in reporter constructs did not modify mRNA levels in transfected cells, which suggested that the increase in expression was due to enhanced translation and not increased transcription or mRNA stability.

Deletion analysis of apoB 5′UTR was performed to assess potential sequence elements that confer its stimulatory effect on the luciferase reporter or apoB15 observed above. Data obtained from deletion experiments must be interpreted cautiously. This is due to the fact that excision of even a relatively small sequence may result in a substantial reorganization of the secondary structure of the corresponding deletion mutation segment, resulting in an RNA structure which has little in common with the original or wild-type RNA structure. A similar conclusion was made by Rubtsova et al. (*28*). We thus have attempted to interpret the results on the basis of the predicted secondary structures of the deletion mutants in comparison with the wild-type apoB 1−128 5′UTR RNA structure. Nucleotides 3−13, 21−67, and 69−90 correspond to hairpins 1, 2, and 3, respectively, from the predicted secondary structure of the apoB 5′UTR. The 5′UTR 1−96 construct, which had an activity similar to the wild-type full-length 1−128 levels, contained both hairpins 2 and 3 and the first 32 5′ nucleotides which may be important for optimal translation. Deletion of sequences involved in the formation of one or more of these hairpin structures appeared to abolish the stimulatory effect of the 5′UTR on translational activity. We thus hypothesize that hairpins 1, 2, and 3 are vital for cis−trans interactions which mediate translational control of the apoB mRNA since deletion of either hairpin causes a loss of optimal translation.

We postulate that the stem-loop structures noted from the secondary structure predictions may be potential binding sites for eukaryotic initiation factors or other RNA-binding proteins whose function is to alleviate or relax the secondary structure present in the 5′UTR. For example, initiation factor eIF4A, upon activation by eIF4B, may unwind highly structured 5′UTR's through its ATP-dependent RNA helicase activity and decrease the repression imposed by secondary structure (*14*). Protein factors may recruit translational machinery, unwind secondary structure, or increase mRNA stability, thus contributing to efficient translation of the apoB message. Such an occurrence is observed in the 5′UTR-mediated efficient translation of p27 mRNA. This region contains a U-rich sequence that forms secondary structure which has been shown to bind the protein factor HuR, a protein that has been implicated in mRNA stability and translation (*29*). This finding presents an interesting possibility that merits further investigation in our system. Alternatively, the apoB message may be translated via internal ribosomal entry sites. The 5′UTR of apoB is highly structured and has a stable Y-shaped secondary structure with the presence of a small stem loop (in five of the seven Y-shaped predictions) at the 3′ end of the leader. Thus some of the structural features exhibited in the apoB 5′UTR are consistent with RNA structural motifs common to other cellular mRNAs that use this mechanism for translation (*30*). The features or criteria that are not consistent with other cellular mRNAs are that the 5′UTR of apoB is relatively short and does not possess upstream AUGs. Since our data indicated that the presence of the 5′UTR results in increased LUC expression, this is one potential mechanism by which the apoB mRNA may be translated efficiently. Further studies are necessary to elucidate such mechanisms.

REFERENCES

1. Brunzell, J. D., Sniderman, A. D., Albers, J. J., and Kwiterovich, P. O., Jr. (1984) Apoproteins B and A-I and coronary artery disease in humans, *Arteriosclerosis 4*, 79−83.
2. Knott, T. J., Pease, R. J., Powell, L. M., Wallis, S. C., Rall, S. C., Jr., Innerarity, T. L., Blackhart, B., Taylor, W. H., Marcel, Y., Milne, R., et al. (1986) Complete protein sequence and identification of structural domains of human apolipoprotein B, *Nature 323*, 734−738.
3. Yao, Z., and McLeod, R. S. (1994) Synthesis and secretion of hepatic apolipoprotein B-containing lipoproteins, *Biochim. Biophys. Acta 1212*, 152−166.
4. Lusis, A. J., Taylor, B. A., Quon, D., Zollman, S., and LeBoeuf, R. C. (1987) Genetic factors controlling structure and expression of apolipoproteins B and E in mice, *J. Biol. Chem. 262*, 7594−7604.
5. Dashti, N., Williams, D. L., and Alaupovic, P. (1989) Effects of oleate and insulin on the production rates and cellular mRNA concentrations of apolipoproteins in HepG2 cells, *J. Lipid Res. 30*, 1365−1373.
6. Kaptein, A., Roodenburg, L., and Princen, H. M. (1991) Butyrate stimulates the secretion of apolipoprotein (apo) A-I and apo B100 by the human hepatoma cell line Hep G2. Induction of apo A-I mRNA with no change of apo B100 mRNA, *Biochem. J. 278*, 557−564.
7. Moberly, J. B., Cole, T. G., Alpers, D. H., and Schonfeld, G. (1990) Oleic acid stimulation of apolipoprotein B secretion from HepG2 and Caco-2 cells occurs posttranscriptionally, *Biochim. Biophys. Acta 1042*, 70−80.
8. Pullinger, C. R., North, J. D., Teng, B. B., Rifici, V. A., Ronhild de Brito, A. E., and Scott, J. (1989) The apolipoprotein B gene is constitutively expressed in HepG2 cells: regulation of secretion by oleic acid, albumin, and insulin, and measurement of the mRNA half-life, *J. Lipid Res. 30*, 1065−1077.
9. Adeli, K., and Theriault, A. (1992) Insulin modulation of human apolipoprotein B mRNA translation: studies in an in vitro cell-free system from HepG2 cells, *Biochem. Cell Biol. 70*, 1301−1312.
10. Theriault, A., Ogbonna, G., and Adeli, K. (1992) Thyroid hormone modulates apolipoprotein B gene expression in HepG2 cells, *Biochem. Biophys. Res. Commun. 186*, 617−623.
11. Sparks, J. D., and Sparks, C. E. (1990) Insulin modulation of hepatic synthesis and secretion of apolipoprotein B by rat hepatocytes, *J. Biol. Chem. 265*, 8854−8862.
12. Sparks, J. D., Zolfaghari, R., Sparks, C. E., Smith, H. C., and Fisher, E. A. (1992) Impaired hepatic apolipoprotein B and E translation in streptozotocin diabetic rats, *J. Clin. Invest. 89*, 1418−1430.
13. Day, D. A., and Tuite, M. F. (1998) Post-transcriptional gene regulatory mechanisms in eukaryotes: an overview, *J. Endocrinol. 157*, 361−371.
14. van der Velden, A. W., and Thomas, A. A. (1999) The role of the 5′ untranslated region of an mRNA in translation regulation during development, *Int. J. Biochem. Cell Biol. 31*, 87−106.
15. Jansen, R. P. (2001) mRNA localization: message on the move, *Nat. Rev. Mol. Cell. Biol. 2*, 247−256.
16. Bashirullah, A., Cooperstock, R. L., and Lipshitz, H. D. (2001) Spatial and temporal control of RNA stability, *Proc. Natl. Acad. Sci. U.S.A. 98*, 7025−7028.
17. McCarthy, J. E., and Kollmus, H. (1995) Cytoplasmic mRNA-protein interactions in eukaryotic gene expression, *Trends Biochem. Sci. 20*, 191−197.
18. Knott, T. J., Wallis, S. C., Powell, L. M., Pease, R. J., Lusis, A. J., Blackhart, B., McCarthy, B. J., Mahley, R. W., Levy-Wilson, B., and Scott, J. (1986) Complete cDNA and derived protein sequence of human apolipoprotein B-100, *Nucleic Acids Res. 14*, 7501−7503.
19. Kozak, M. (1991) Structural features in eukaryotic mRNAs that modulate the initiation of translation, *J. Biol. Chem. 266*, 19867−19870.
20. Kozak, M. (1989) Circumstances and mechanisms of inhibition of translation by secondary structure in eucaryotic mRNAs, *Mol. Cell. Biol. 9*, 5134−5142.
21. Zuker, M. (1989) Computer prediction of RNA structure, *Methods Enzymol. 180*, 262−288.
22. Jaeger, J. A., Turner, D. H., and Zuker, M. (1989) Improved predictions of secondary structures for RNA, *Proc. Natl. Acad. Sci. U.S.A. 86*, 7706−7710.
23. Jaeger, J. A., Turner, D. H., and Zuker, M. (1990) Predicting optimal and suboptimal secondary structure for RNA, *Methods Enzymol. 183*, 281−306.
24. Adeli, K. (1994) Regulated intracellular degradation of apolipoprotein B in semipermeable HepG2 cells, *J. Biol. Chem. 269*, 9166−9175.
25. Taghibiglou, C., Rashid-Kolvear, F., Van Iderstine, S. C., Le Tien, H., Fantus, I. G., Lewis, G. F., and Adeli, K. (2002) Hepatic very low density lipoprotein-ApoB overproduction is associated with attenuated hepatic insulin signaling and overexpression of protein-tyrosine phosphatase 1B in a fructose-fed hamster model of insulin resistance, *J. Biol. Chem. 277*, 793−803.
26. Kozak, M. (1989) The scanning model for translation: an update, *J. Cell Biol. 108*, 229−241.
27. Vivinus, S., Baulande, S., Van Zanten, M., Campbell, F., Topley, P., Ellis, J. H., Dessen, P., and Coste, H. (2001) An element within the 5′ untranslated region of human Hsp70 mRNA which acts as a general enhancer of mRNA translation, *Eur. J. Biochem. 268*, 1908−1917.
28. Rubtsova, M. P., Sizova, D. V., Dmitriev, S. E., Ivanov, D. S., Prassolov, V. S., and Shatsky, I. N. (2003) Distinctive properties of the 5′-untranslated region of human hsp70 mRNA, *J. Biol. Chem. 278*, 22350−22356.
29. Millard, S. S., Vidal, A., Markus, M., and Koff, A. (2000) A U-rich element in the 5′ untranslated region is necessary for the translation of p27 mRNA, *Mol. Cell. Biol. 20*, 5947−5959.
30. Le, S. Y., and Maizel, J. V., Jr. (1997) A common RNA structural motif involved in the internal initiation of translation of cellular mRNAs, *Nucleic Acids Res. 25*, 362−369.

BI049887S